phosphonate, the $[M - C_2H_4O]^{+\cdot}$ ion of triethyl phosphate and the $[M - C_2H_4]^{+\cdot}$ ion of triethyl phosphite) all produce nearly identical breakdown graphs even under single-collision conditions (Table III). The lowest known activation energy for the fragmentation of the $[M - C_2H_4O]^{+\cdot}$ ion of triethyl phosphate is 1.9 eV,[19] corresponding to the loss of C_2H_4, and this is probably the lowest energy process for this ion (the activation energy for the other favored reaction, loss of $C_2H_3\cdot$, is 2.0 eV).[19] This activation energy is much higher than the fragmentation threshold of dimethyl phosphonate ion (d) and its tautomer (c) (0.7 and 1.3 eV, respectively), which makes it more probable in the former case that the isomerization barrier is below the fragmentation thresholds of the tautomers. Indeed, the results obtained for the ethyl homologues indicate that isomerization to a common structure or mixture of structures occurs *prior to* decomposition.[31] This is contrary to the behavior of the methyl homologues, which retain their structural identity under the same experimental conditions.

Conclusion

Ionized dimethyl phosphite is significantly more stable than the phosphonate tautomer, in striking contrast to the relative stabilities of the corresponding neutral molecules. This stability difference, as well as the preferred formation of the more stable of these tautomers in the fragmentation of ionized trimethyl phosphate, supports and rationalizes the earlier evidence[11,23] of a very strong tendency of organophosphorus ester ions for formation of the P–OH group. One of the forces driving gas-phase reactions of ionized phosphorus esters seems to be generation of the P–OH structure, whereas P=O bond formation plays a corresponding role in reactions of neutral phosphorus esters. In contrast to the behavior of the methyl tautomers, ionized diethyl phosphonate and phosphite tautomers are not distinguishable, and available thermochemical data explain this.

This work clearly demonstrates the capability of energy-resolved mass spectrometry in differentiating tautomeric ion structures. In addition, the results show the importance of using low target pressures in collision-induced dissociation when closely similar ion structures are compared. Because of enhanced isomerization under multiple-collision conditions, structural identity of ionized dimethyl phosphonate and dimethyl phosphite is lost.

Even in such simple systems as studied here, the ion chemistry is surprisingly rich. Additional mass spectrometric techniques now emerging, such as the ability to carry out sequential collision-induced dissociations by utilizing collision chambers situated in different parts of a tandem mass spectrometer,[32] will be useful in further research on the phenomena revealed here.

Acknowledgment. This work was supported by the National Science Foundation, No. CHE 80-11425. The support provided by the Academy of Finland is gratefully acknowledged (H.K.).

Registry No. Dimethyl phosphonate, 13598-36-2; dimethyl phosphonate ion, 95120-13-1.

(31) The breakdown graph obtained for the molecular ion of diethyl phosphonate shows a slightly more intense peak at m/z 111 than do the ions with the same composition obtained from different sources. The formation of m/z 111 (loss of $C_2H_3\cdot$) requires two hydrogen shifts. It fragments further to m/z 83. The formation of all the other abundant ions (m/z 110, 82; see Table III) requires a single hydrogen shift. Furthermore, the corresponding peaks are only minor or totally absent in the electron impact ionization mass spectrum of diethyl phosphonate (see ref 30), although the energy resolved mass spectrometry experiment showed them to arise from high-energy processes (which usually produce more abundant peaks to electron impact ionization mass spectra than low-energy CID spectra), thus indicating that they, in fact, are the result of a preceding slow isomerization g → h. In the ion source, because of competition between fast direct bond cleavages and rearrangement reactions, isomerization does not occur to a significant extent. Thus, it can be concluded that also here, as in the case of c and d, fragmentation via hydrogen transfers is preferred for the phosphonate structure.

(32) Burinsky, D. I.; Cooks, R. G.; Chess, E. K.; Gross, M. L. *Anal. Chem.* **1982**, *54*, 295.

Electron Spin Resonance Study of Tris[2-aminobenzenethiolato(2-)-*S*,*N*]technetium(VI) and -rhenium(VI) Chelates: Evidence for Molecular Aggregation in Solution

John Baldas,[†] John F. Boas,*[†] John Bonnyman,[†] John R. Pilbrow,[‡] and Geoffrey A. Williams[†]

Contribution from the Australian Radiation Laboratory, Yallambie, Victoria, 3085 Australia, and the Department of Physics, Monash University, Clayton, Victoria, 3168 Australia.
Received July 10, 1984

Abstract: ESR measurements at ca. 9.15 GHz and in the range 2–4 GHz have enabled the effects of concentration and solvent composition on the spectra of frozen solutions of trigonal-prismatic tris[2-aminobenzenethiolato(2-)-*S*,*N*]technetium(VI) and -rhenium(VI) complexes to be interpreted in terms of the breakdown of molecular aggregates. In the case of $Tc(abt)_3$, this dissociation gives the monomeric species, while $Re(abt)_3$ appears to give a mixture of trimeric and monomeric species. The spectra arising from the monomeric species are best interpreted by almost isotropic g and A values but with a subtle interplay of anisotropic line width effects. The extent of the delocalization of the unpaired electron in the $2a_2'$ molecular orbital onto the ligands is indicated by the effects on the ESR spectra of intermolecular exchange interactions between $Re(abt)_3$ molecules, where the Re ions are probably ca. 10 Å apart. This is a rare example of intermolecular exchange interactions without a direct-bonded pathway.

The use of technetium compounds as radiopharmaceuticals has stimulated interest in the physical and chemical properties of technetium complexes in general. In addition, the location of technetium in the periodic table between molybdenum and ruthenium along the 4d transition series and with the same d electron configuration as manganese (3d) and rhenium (5d) enables comparisons to be made between the behavior of technetium and these other chemically very interesting metallic elements.

An X-ray diffraction study of the complex tris[2-aminobenzenethiolato(2-)-*S*,*N*]technetium(VI), $Tc(abt)_3$ (I), showed that the technetium ion was six-coordinate in a trigonal-prismatic

[†] Australian Radiation Laboratory.
[‡] Monash University.

0002-7863/85/1507-1886$01.50/0

configuration and that $Tc(abt)_3$ was isomorphous with $Mo(abt)_3$.[1]

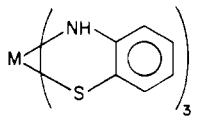

I M = Tc
II M = Re

Trigonal-prismatic geometry has also been found to occur for a number of dithiolate complexes of molybdenum, tungsten, and rhenium where the metal is bonded to six sulfur atoms, e.g., the Mo, W, and Re complexes of tris(*cis*-1,2-diphenylethene-1,2-dithiolate), $M(S_2C_2Ph_2)_3$,[2a,b,3] tris(toluene-3,4-dithiolate), $M(tdt)_3$,[3] and tris(benzene-1,2-dithiolate), $M(bdt)_3$.[4] The unusual coordination geometry has led to considerable controversy as to whether the ground state configuration is of the type $(3a_1')^2(4e')^4(5e')^1$, $(4e')^4(2a_2')^2(3a_1')^1$, or $(3a_1')^2(4e')^4(2a_2')^1$.[4-9] The first two configurations have significant metal character, whilst the third implies that the unpaired electron is in a ligand orbital.

In principle, electron spin resonance measurements should provide information as to the nature of the ground state. However previous studies of the ESR spectra of $Tc(tdt)_3$,[8] $Tc(abt)_3$,[9] $Re(tdt)_3$,[7,8] $Re(abt)_3$ (II),[9] and $Re(S_2C_2Ph_2)_3$[5,7] in nonaqueous solutions exhibited either a single line at g ca. 2 or a series of poorly resolved lines in the same region. The latter spectra were interpreted in terms of a species with anisotropic g values (typically $g_1 = 2.05$, $g_2 = 2.01$, $g_3 = 1.98$) and a small anisotropic hyperfine structure with $A \lesssim 0.001$ cm^{-1}. These g and, more particularly, hyperfine values may be contrasted with those observed for Tc and Re in a tetragonal environment, where the hyperfine values may be some 2 orders of magnitude larger.[10,11] The ESR parameters of paramagnetic species such as those produced by the reduction of $Mo(abt)_3$ were similar to those expected from the metal ion in nearly octahedral or tetrahedral environments.[12]

It was thought that it might be possible to obtain much better resolved spectra of $Tc(abt)_3$ and $Re(abt)_3$ by a judicious choice of solvent and by a decrease in solute concentration. Furthermore, the combination of measurements at the usual X-band frequencies (ca. 9.15 GHz) and at lower frequencies such as the S band (2–4 GHz) should enable features arising from g-value anisotropy, which will spread over a range of magnetic field proportional to the microwave frequency, to be distinguished from those due to field-independent interactions such as hyperfine effects or dipole–dipole and weak exchange coupling.[13] A reduction in microwave frequency may also help to resolve features which are obscured by strain broadening effects at high frequencies. Our results show that the unpaired electron in these systems is delocalized over the entire π system of the ligands, leading, in the case of $Re(abt)_3$, to manifestations of exchange interactions between adjacent molecules in frozen solution.

Experimental Section

$Tc(abt)_3$ was prepared as described by Baldas et al.[1] and $Re(abt)_3$ as described by Gardner et al.[12] Analytical grade solvents were used without further purification.

The ESR spectra, recorded as the first derivatives of absorption, were obtained by using a Varian E-12 spectrometer with an E-101 microwave bridge at the X band (ca. 9.15 GHz) and a home-built S-band microwave bridge. A large rectangular sample cavity (25 × 10 × 2.5 cm) operating at ca. 2, ca. 2.9, and ca. 4 GHz was used. Low temperatures were achieved by means of a Varian E-257 variable-temperature accessory (above ca. 100 K), at liquid-nitrogen temperature by using narrow-tail quartz Dewar flasks and at 10 K by using an Oxford Instruments continuous-flow helium cryostat. Magnetic fields were calibrated against proton NMR frequencies measured by using a Hewlett-Packard HP 5254 L frequency counter. Microwave frequencies above 3 GHz were measured by using a Hewlett-Packard HP 540B microwave mixer and counter, while below 3 GHz they were measured with the aid of a 0.2–3-GHz H5254B plug-in unit on the counter.

Spectra due to monomeric species were interpreted by use of the spin Hamiltonian for orthorhombic systems, simplified where appropriate for axial or isotropic systems, namely

$$\mathcal{H} = \beta[B_x g_x S_x + B_y g_y S_y + B_z g_z S_z] + A_x S_x I_x + A_y S_y I_y + A_z S_z I_z \quad (1)$$

where $S = {}^1/_2$ and $I = {}^9/_2$ (Tc) or ${}^5/_2$ (Re). Preliminary computer simulations were carried out by using the program MONOCLIN.[14] Final monomer simulations were carried out by using a modified version of MONOCLIN (MONOQF) in which the g–A strain contributions to the line widths of different hyperfine components in the spectrum are readily taken into account.[15]

MONOQF differs from conventional algorithms in that the line shape function is written as

$$f(\nu_c - \nu_o(B), \sigma_\nu) \quad (2)$$

where ν_c is the fixed microwave frequency and $h\nu_o(B)$ the energy difference between the levels as a function of magnetic field. The line shape parameter

$$\sigma_\nu = [\sigma_R^2 + (c_1\nu_o(B) - c_2 m)^2]^{1/2} \quad (3)$$

is a modification of a similar result where the terms have magnetic field units. The advantage of (3) is that the resulting line shape in a field-swept experiment may not be symmetric. Following Hyde and Froncisz,[13] it can be shown that

$$c_1 = \Delta g / g \quad (4)$$

and

$$c_2 = -\Delta A / h$$

where Δg and ΔA represent Gaussian half-widths of g- and A-strain broadening effects. It is assumed that the resulting line width is Gaussian and arises from a convolution of a residual line (width σ_R) and the g–A strain contributions involving c_1 and c_2. Equation 3 provides a consistent means of interpreting the observed dependence of the line width on the microwave frequency and the nuclear quantum number, m.

The possible involvement of dimeric species was evaluated by using the program GNDIMER, which includes terms to account for small exchange interactions as described by Smith and Pilbrow.[16] The spin Hamiltonian used here for a pair of ions has the form

$$\mathcal{H} = \mathcal{H}_1 + \mathcal{H}_2 + \mathcal{H}_d - JS_1 \cdot S_2 \quad (5)$$

where $\mathcal{H}_1$ and $\mathcal{H}_2$ are the spin Hamiltonians of the individual ions, $\mathcal{H}_d$ represents the dipolar coupling Hamiltonian, and the term $JS_1 \cdot S_2$ represents the isotropic-exchange coupling interaction between the ions of spins S_1 and S_2. In the present case, $S_1 = S_2 = {}^1/_2$. The version of GNDIMER used for this paper incorporates symmetric component line shapes rather than the possible asymmetric lines implied by eq 2–4.

It is also necessary to consider the ESR spectra which would arise from trimeric clusters. The background theory has been given by Harris and Owen[17] who describe the exchange interactions between the components of a trimer in terms of two isotropic exchange parameters. When three paramagnetic ions each with spin $S = {}^1/_2$ are coupled together, two spin doublets ($S = {}^1/_2$) and a spin quartet ($S = {}^3/_2$) result. In the

(1) Baldas, J.; Boas, J. F.; Bonnyman, J.; Mackay, M. F.; Williams, G. A. *Aust. J. Chem.* **1982**, *35*, 2413.
(2) (a) Eisenberg, R.; Ibers, J. A. *J. Am. Chem. Soc.* **1965**, *87*, 3776. (b) Eisenberg, R.; Ibers, J. A. *Inorg. Chem.* **1966**, *5*, 411.
(3) Stiefel, E. I.; Gray, H. B. *J. Am. Chem. Soc.* **1965**, *87*, 4012.
(4) Bennett, M. J.; Cowie, M.; Martin, J. L.; Takats, J. *J. Am. Chem. Soc.* **1973**, *75*, 7504.
(5) Stiefel, E. I.; Eisenberg, R.; Rosenberg, R. C.; Gray, H. B. *J. Am. Chem. Soc.* **1966**, *88*, 2956.
(6) Schrauzer, G. N.; Mayweg, V. P. *J. Am. Chem. Soc.* **1966**, *88*, 3235.
(7) Al-Mowali, A. H.; Porte, A. L. *J. Chem. Soc., Dalton Trans.* **1975**, 250.
(8) Kawashima, M.; Koyama, M.; Fujinaga, T. *J. Inorg. Nucl. Chem.* **1976**, *38*, 801.
(9) Kirmse, R.; Stach, J.; Spies, H. *Inorg. Chim. Acta* **1980**, *45*, L251.
(10) Baldas, J.; Boas, J. F.; Bonnyman, J.; Williams, G. A. *J. Chem. Soc., Dalton Trans.* **1984**, 2395.
(11) Lack, G. M.; Gibson, J. F. *J. Mol. Struct.* **1978**, *46*, 299.
(12) Gardner, J. K.; Pariyadath, N.; Corbin, J. L.; Stiefel, E. I. *Inorg. Chem.* **1978**, *17*, 897.
(13) Hyde, J. S.; Froncisz, W. *J. Chem. Phys.* **1980**, *73*, 3132; *Annu. Rev. Biophys. Bioeng.* **1982**, *11*, 391.
(14) Pilbrow, J. R.; Winfield, M. E. *Mol. Phys.* **1973**, *25*, 1073.
(15) Pilbrow, J. R. *J. Magn. Reson.* **1984**, *58*, 186.
(16) Smith, T. D.; Pilbrow, J. R. *Coord. Chem. Rev.* **1974**, *13*, 173.
(17) Harris, E. A.; Owen, J. *Proc. R. Soc. London, Ser. A* **1965**, *289*, 122.

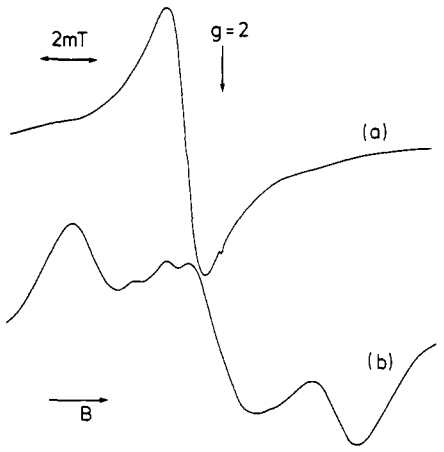

Figure 1. ESR spectra at 9.139 GHz of $Tc(abt)_3$ in frozen solution (120 K): (a) 1×10^{-3} M in $CHCl_3$, 0.05-mT modulation amplitude, 5-mW microwave power, 0.1-s time constant, 2.5×10^2 gain, 5 mT/min scan rate; (b) 5×10^{-4} M in $CHCl_3$, 0.1-mT modulation amplitude, 20-mW microwave power, 0.1-s time constant, 2.5 mT/min scan rate, 8.0×10^2 gain.

simplest case, the ESR spectra from the spin doublets will consist of an isotropic line at g ca 2. The ESR spectra of the quartet can be described by the spin Hamiltonian

$$\mathcal{H} = g\beta B \cdot S + D(S_z^2 - \tfrac{1}{3}S(S+1)) \quad (6)$$

where $S = {}^3/_2$ and D is not simply related to the splitting between the quartet and the doublets. The allowed transitions for any single orientation of the magnetic field with respect to the trimer axis will consist of three equally spaced lines centered at g ca.2 and with intensity ratios 3:4:3.

In order to simulate frozen solution spectra when $D \ll g\beta B$, the expressions for the magnetic field in MONOQF were modified by the first-order expression

$$B = B_0 - D(3\cos^2\theta - 1)(M - \tfrac{1}{2})/g\beta \quad (7)$$

where $B_0 = (h\nu)/(g\beta)$ and θ is the angle between the magnetic field and the symmetry of the zero-field-splitting tensor of the quartet state. By setting $M = {}^3/_2$, ${}^1/_2$, and $-{}^1/_2$ in turn, all three $\Delta M = \pm 1$ transitions are accounted for.

ESR Results and Interpretation

$Tc(abt)_3$. At room temperature and microwave frequencies of ca. 9 GHz, a 2×10^{-4} M solution in benzene exhibited a single resonance at $g = 2.007$ with a peak-to-peak line width of 4.2 mT.

In frozen solution (120 K), the spectrum depended on both the solute concentration and the solvent composition. At 1×10^{-3} M in chloroform, the main feature was an intense line at $g = 2.007$ with a peak-to-peak width of 1.3 mT, as shown in Figure 1a. Poorly resolved shoulders are present at fields of ca. 4 mT either side of the main peak. Dilution of this solution to 5×10^{-4} M resulted in the spectrum shown in Figure 1b, which is similar to that reported by Kirmse et al.[9] for this concentration. The central resonance has decreased in intensity, whilst the shoulders have become better resolved and some structure has appeared in the central region. After dilution to 2×10^{-4} M, the central resonance was almost completely absent and both the shoulders and the structure in the central region were well resolved. The best resolved spectra at 2×10^{-4} M were obtained when the solvent contained a high proportion of a coordinating solvent such as pyridine or dimethylformamide. The spectrum obtained in a dimethylformamide–chloroform mixture (9:1 v/v) is shown in Figure 2a. No further resolution could be obtained in a more dilute solution. In all cases no resonances additional to those described above were observed at magnetic fields between 0 and 450 mT, even though the spectrometer gain was such that signals 1000 times weaker than the main resonances could have been detected. The spectra were unchanged by a reduction in sample temperature to 10 K.

The spectral behavior as a result of dilution and change of solvent composition is reminiscent of that observed for some

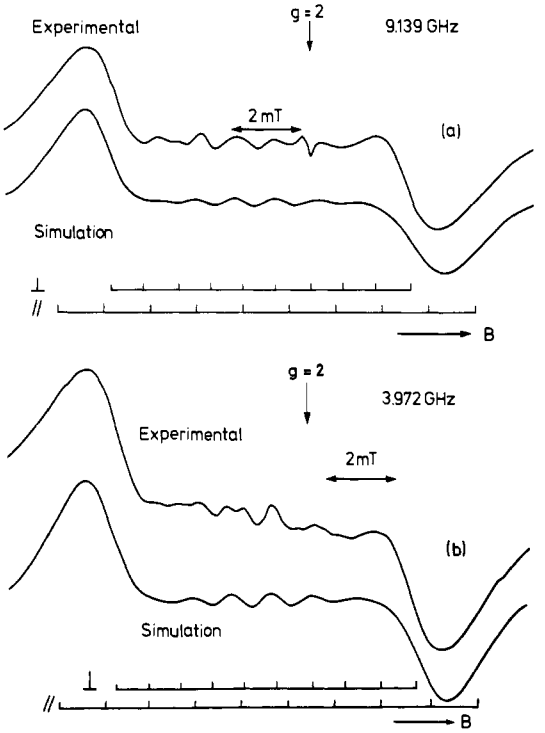

Figure 2. Experimental and simulated ESR spectra of 2×10^{-4} M $Tc(abt)_3$ in frozen 9:1 $DMF/CHCl_3$ at (a) 9.139 GHz and 120 K (0.2-mT modulation amplitude, 5-mW microwave power, 0.1-s time constant, 5 mT/min scan rate, 6.3×10^2 gain) and (b) 3.972 GHz and 10 K (2-mT nominal modulation amplitude, 0.5-s time constant, 5 mT/min scan rate, 3.2×10^3 gain, microwave power level—Engleman CC24 oscillator at full power). Spectra were simulated by use of the parameters given in Table I. The positions of the perpendicular and parallel features are shown underneath the simulated spectrum. The sharp feature observed near $g = 2$ in (a) is due to a background free-radical signal.

porphyrin and phthalocyanine complexes. For example, the addition of dimethylformamide to an aqueous solution of some copper(II) porphyrins and phthalocyanines results in the breakdown of polymeric species, as identified by the observation in the ESR experiment of a relatively narrow line near $g = 2$, to smaller aggregates, e.g., dimers and eventually, to monomers,[18-20] each with quite distinctive ESR signals. In the present case, the signal observed at 1×10^{-3} M in chloroform is explained as arising from aggregates of $Tc(abt)_3$ molecules, where the isotropic line shape arises from the cumulative effect of the magnetic dipole–dipole and weak electronic-exchange interactions between a large number of molecules. The species represented by the signal shown in Figure 2a is then the result of the breakdown of the aggregate.

The spectra observed at 10 K and microwave frequencies of 2.896 and 3.972 GHz are virtually identical with those observed at around 9 GHz and show that the spectral features must arise from hyperfine interactions or small zero field splittings. Such features are expected to remain essentially unaffected by the decrease in microwave frequency. The spectrum of $Tc(abt)_3$ at 2×10^{-4} M concentration in dimethylformamide–chloroform (9:1 v/v) at 10 K and 3.972 GHz is shown in Figure 2b. The most straightforward explanation of the ESR spectra of Figure 2 is that they arise from a monomeric species and that the unpaired electron in $Tc(abt)_3$ is so highly delocalized away from the Tc nucleus that both g and A are almost isotropic and A is quite small. The low-frequency experiments show that a model based on more anisotropic g values, such as those used by Kirmse et al.,[9] cannot be correct.

(18) De Bolfo, J. A.; Smith, T. D.; Boas, J. F.; Pilbrow, J. R. *J. Chem. Soc., Dalton Trans.* **1975**, 1523.
(19) De Bolfo, J. A.; Smith, T. D.; Boas, J. F.; Pilbrow, J. R. *J. Chem. Soc., Faraday Trans. 2* **1976**, 481.
(20) Chikira, M.; Kon, H.; Hawley, R. A.; Smith, K. M. *J. Chem. Soc., Dalton Trans.* **1979**, 245.

Table I. ESR Parameters for $Tc(abt)_3$ and $Re(abt)_3$

		$Tc(abt)_3$		
		parallel	perpendicular	$Re(abt)_3$
	g	2.0073 ± 0.0002	2.0080 ± 0.0002	2.009
	A, (10^{-4} cm^{-1})	12.2 ± 0.2	8.7 ± 0.2	19
residual line width	σ_R, MHz	19.0 ± 1.0	15.3 ± 1.0	45
g-strain parameter	c_1	0.0001 ± 0.0001	0.0005 ± 0.0001	
A-strain parameter	c_2, MHz	2.1 ± 0.1	2.1 ± 0.1	

The resonances shown in Figure 2 cannot arise from dimeric species for the following reasons. Firstly, if the Tc···Tc distance was less than about 7.5 Å, a computer simulation assuming similar line widths to those found in the $g = 2$ region of the monomer shows that a resonance at around 160 mT due to the forbidden ($\Delta M = 2$) transitions should be observed. No signals were found in this region for any of the spectra discussed in this paper. Secondly, computer simulations using GNDIMER and including exchange coupling and/or dipolar coupling involving two Tc ions at distances larger than ca. 7.5 Å were not able to reproduce the experimental spectra.

Thus we may conclude that the effect of dilution and addition of more strongly coordinating solvents to solutions of $Tc(abt)_3$ is to break down the polymeric aggregate found at high solute concentrations to a monomeric species, without the formation of a stable dimeric species. Since we were unable to observe spectra from dimeric species and have no a priori information as to their line widths, we are unable to put an upper limit on their possible concentration.

The value of obtaining spectra at more than one microwave frequency was shown during the computer simulation of the spectra. Although the essential correctness of the almost isotropic g and A model was confirmed by the initial simulations of the 9-GHz spectra, the low-frequency spectra were easier to simulate. The 9-GHz spectra were then checked by using the same spectral parameters, and this procedure provided upper limits for the deviation of g and A from axial symmetry. The parameters are given in Table I, and spectra simulated by using these values are also shown in Figure 2. The simulations show that the peculiar shape of the spectra, when recorded as the first derivative of the absorption, arise because the widths of the individual hyperfine lines are approximately the same as the hyperfine splittings. The resolution of the peaks in the central region then depends on the overlap of the component lines. The simulations also show that the poorly resolved features observed by Kirmse et al.[9] (cf. Figure 1b) arise from Tc hyperfine interactions and not from superhyperfine interactions with the neighboring nitrogen nuclei or protons on the ring system. The effect of eq 3 on the component line widths is shown in Table II. It will be noticed that the line widths decrease toward the center of the spectrum, as required for adequate simulation of the experimental spectrum. No assumptions are made in eq 3 as to whether the line shapes are symmetric or not in field-swept ESR.

Re(abt)$_3$. Solutions of $Re(abt)_3$ in benzene at room temperature exhibited a single isotropic line of peak-to-peak width 11.2 mT at $g = 2.009$ at ca. 9-GHz microwave frequency. Solutions of $Re(abt)_3$ at solute concentrations of 1×10^{-3} M in benzene or dimethyl sulfoxide, frozen to 120 K, also exhibited only a single isotropic resonance at $g = 2.009$ but with a smaller line width, namely ca. 3.0 mT as shown in Figure 3a. At solute concentrations of ca. 1×10^{-4} M, a microwave frequency of 9.139 GHz, and a temperature of 120 K, the spectra of $Re(abt)_3$ in a variety of solvents consisted of the narrow resonance described above and two partially resolved shoulders, one on either side of the central line and ca. 11 mT apart, as shown in Figure 3b. The appearance of this spectrum was not changed either by dilution to 10^{-5} M or by changes in solvent composition and is similar to the spectra reported by Kirmse et al.[9] for $Re(abt)_3$. Similar spectra have been reported by Al-Mowali and Porte[7] for $Re(tdt)_3$ and $Re(S_2C_2Ph_2)_3$ but have different splittings of the shoulder features.

The spectra observed at microwave frequencies of 3.9719, 2.8695, and 1.980 GHz and at 77 and 10 K are identical with those observed at 9.139 GHz and 120 K, showing that, as with $Tc(abt)_3$, the main features are due to frequency-independent splittings. The spectrum at 1.980 GHz and 10 K is shown in Figure 3c.

The spectra may be interpreted in the same way as those of $Tc(abt)_3$, with the isotropic line of Figure 3a arising from a polymeric species. The shoulders observed on either side of the central resonance are then interpreted as being due to a monomeric species, with isotropic g and hyperfine values. The parameters giving the best fit to this part of the experimental spectrum are given in Table I. The resolution of this spectrum was not sufficient

Table II. Theoretical Line Widths (in MHz) for $Tc(abt)_3$[a]

	microwave frequency ν_c, GHz	
m[b]	9.139	3.972
	Parallel	
$^9/_2$	20.8	21.0
$^7/_2$	20.1	20.2
$^5/_2$	19.5	19.6
$^3/_2$	19.1	19.2
$^1/_2$	19.0	19.0
$-^1/_2$	19.1	19.1
$-^3/_2$	19.4	19.3
$-^5/_2$	20.0	19.8
$-^7/_2$	20.7	20.5
$-^9/_2$	21.6	21.4
	Perpendicular	
$^9/_2$	16.1	17.0
$^7/_2$	15.6	16.2
$^5/_2$	15.3	15.6
$^3/_2$	15.4	15.3
$^1/_2$	15.7	15.3
$-^1/_2$	16.3	15.6
$-^3/_2$	17.1	16.0
$-^5/_2$	18.2	16.9
$-^7/_2$	19.4	17.9
$-^9/_2$	20.8	19.1

[a] To convert values to millitesla divide parallel widths by 28.1 and perpendicular widths by 28.0. [b] m values given on basis that A values are positive.

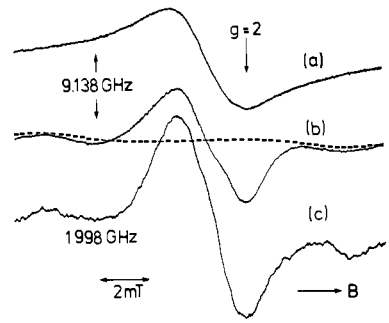

Figure 3. ESR spectra of $Re(abt)_3$ in frozen solution (a) in benzene (ca. 10^{-3} M) at 9.139 GHz and 120 K (0.05-mT modulation amplitude, 5-mW microwave power, 0.1-s time constant, 5 mT/min scan rate, 1.25×10^3 gain), (b) in benzene (1×10^{-4} M) at 9.139 GHz, 120 K (conditions as for (a)) (the spectrum simulated by using the parameters in Table I is shown by the broken line) and (c) in Me_2SO (1×10^{-4} M) at 1.980 GHz and 10 K (3.2-mT nominal modulation amplitude, microwave power level—Engleman CC24 oscillator at full power, 3.2-s time constant, 5 mT/min scan rate, 8.0×10^3 gain).

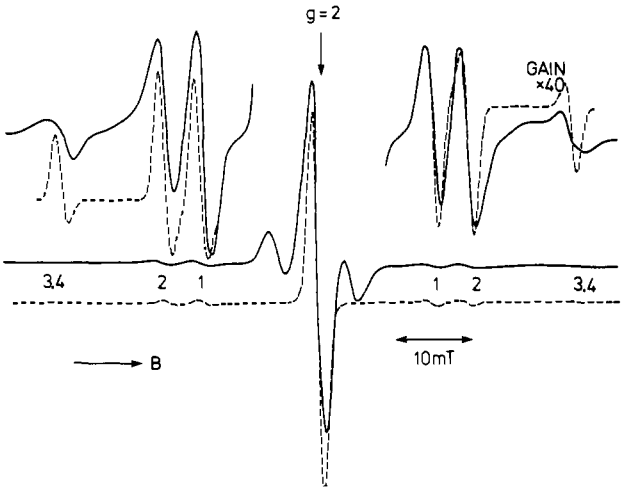

Figure 4. ESR spectrum of $Re(abt)_3$ in frozen solution at 1×10^{-4} M in 50:1 $Me_2SO/CHCl_3$ at 9.142 GHz and 120 K at low and high spectrometer gains. Low gain: 0.2-mT modulation amplitude, 10-mW microwave power, 0.1-s time constant, 12.5 mT/min scan rate, 1.25×10^3 gain. High gain: 1.0-mT modulation amplitude, 40-mW microwave power, 1.0-s time constant, 12.5 mT/min scan rate, 5.0×10^3 gain. (Overall gain is 40 times that at low gain.) The spectrum of the trimeric species, simulated as described in the text, is shown by the broken line. The spectrum in the central region includes the contributions from the doublet states of the trimer, as well as those from the $^1/_2 \rightarrow -^1/_2$ transition of the quartet. The resonances labeled 1–4 represent the $-^3/_2 \rightarrow -^1/_2$ and $^1/_2 \rightarrow {}^3/_2$ transitions within the quartet for $D = 0.0144$, 0.0188, 0.0315, and 0.0325 cm^{-1}, respectively.

to allow an analysis as detailed as that performed for $Tc(abt)_3$ to be carried out.

Further evidence for incomplete disaggregation at low solute concentrations is given by the observation, at high spectrometer gain, of a series of weak satellite lines as shown in Figure 4. The innermost of the satellite lines are equally spaced 15 mT either side of the central line and have an intensity ca. 1% of the central line, the next pair are equally spaced 20 mT either side of the central line and have similar intensity, and the outermost satellites spaced ca. 35 mT either side of the central line have an intensity ca. 0.2% of the central line. These satellite lines are reminiscent of those observed in some systems where there is weak exchange coupling between the paramagnetic centers, e.g., in some vanadyl tartrate binuclear systems,[21] and between a spin label and the metal ion in copper porphyrins.[22]

A possible explanation of the origin of the satellite lines and part of the central feature is that they are due to dimeric species where there are both weak exchange and dipole–dipole interactions between the paramagnetic centers. Computer simulations were carried out by using the program GNDIMER[16] with Re···Re distances of between 9.0 and 10.0 Å, $|J|$ values of 0.013, 0.017, and 0.032 cm^{-1}, and the monomeric g and A values. Whilst it was possible to reproduce the positions and approximate lineshapes of the satellite lines, the central feature had a peak-to-peak width of 5 mT, which is much broader than that observed.

An explanation which reproduces the central feature more accurately is one involving trimeric species. Simulated spectra obtained by using the version of MONOQF based on eq 7 produced the spectra shown in Figure 4, where contributions from species with $D = 0.0144$, 0.0188, 0.0315, and 0.0325 cm^{-1} were added together. In addition, allowance must be made for the contribution to the spectral intensity in the central region from the two spin doublets, which are expected to give a single narrow line at g ca. 2 superimposed on the $^1/_2 \rightarrow -^1/_2$ transitions from the quartet. Part of the contribution to the spectral intensity in this region may also be due to the polymer. The situation is undoubtedly more complicated than that described by this simple model, in view of the fact that we have not been able to reproduce all the details of the satellite line shapes. The resonances 5.6 mT either side of the central line in the $g = 2$ region of the spectra shown in Figures 3 and 4 are due to monomeric species.

The satellite lines could not be positively identified at low microwave frequencies due to insufficient spectrometer sensitivity. Had it been possible to carry out experiments at the Q band (35 GHz), spectra very similar to those at X band would have been observed, as no dependence of satellite intensity on microwave frequency would be expected. A reduction in satellite intensity with increasing microwave frequency is expected if the satellites arise from weakly exchange coupled dimers.

Because both the resonance due to the polymeric species and the satellite lines are observed over a large range of solute concentrations (10^{-3} M down to 10^{-5} M) and in solvents such as ethanol, chloroform, pyridine, benzene, dimethylformamide, dimethyl sulfoxide, and acetonitrile, we conclude that the tendency to depolymerization is much less in solutions of $Re(abt)_3$ than in solutions of $Tc(abt)_3$.

Discussion

The observations of isotropic or almost isotropic g values slightly greater than the free electron value and of hyperfine values an order of magnitude smaller than those found for tetragonal Tc(VI) and Re(VI) complexes indicate that the unpaired electron is in an orbital with mainly ligand character. The present g and A values may be compared with those obtained for the one-electron reduction products of complexes such as $Mo(S_2C_2Ph_2)_3$ and $W(S_2C_2Ph_2)_3$ where the coordination to the metal is also trigonal-prismatic. In these cases, the g values are less than 2.0 and the A values are similar to those for complexes with octahedral or tetragonal symmetry. This implies that the unpaired electron is located in a metal, rather than a ligand, orbital. The fact that two rather than three g and A values are required in the interpretation of the $Tc(abt)_3$ spectrum makes it likely that the parallel axis lies along the approximate trigonal axis of the coordination sphere of the Tc atom. Orientation of the principal g and A values along other directions would lead to a lower symmetry of the paramagnetic complexes.

The possible electronic ground states of trigonal-prismatic Re(VI) complexes have been discussed by Al-Mowali and Porte,[7] who propose the configuration $(3a_1')^2(4e')^4(2a_2')^1$; i.e., the unpaired electron is in the nonbonding $2a_2'$ molecular orbital which is derived from the ligand $3\pi_v$ orbitals. As pointed out by Yamanouchi and Enemark,[23] the interaction of the d_{xy} and $d_{x^2-y^2}$ metal orbitals with the delocalized π_v orbitals is an important factor in the stabilization of trigonal-prismatic geometry. Thus, it is not surprising that $Re(abt)_3$ shows evidence for extreme electron delocalization, and we conclude that both $Re(abt)_3$ and $Tc(abt)_3$ have the same $(2a_2')^1$ configuration as $Re(tdt)_3$ and $Re(S_2C_2Ph_2)_3$ as proposed by Al-Mowali and Porte.[7] The alternative ground states proposed by Schrauzer and Mayweg[6] and Steifel et al.[5] have considerable "metal" character and do not account for the present results.

A consequence of the delocalization of the unpaired electron in $Re(abt)_3$ is the observation of intermolecular-exchange interactions between molecules in solution. Possible pathways for intermolecular exchange may be arrived at if we assume that $Re(abt)_3$ is isomorphous with $Mo(abt)_3$ and $Tc(abt)_3$ and that molecular arrangements in solution are similar to those in the crystalline solid state. Baldas et al.[1] and Yamanouchi and Enemark[23] discuss three types of intermolecular contacts for $Mo(abt)_3$ and $Tc(abt)_3$ in this state.

The first type of intermolecular contact is between some of the atoms of the coordination spheres of neighboring molecules[1] where, in the case of $Tc(abt)_3$, the Tc···Tc distance is 6.05 Å. The ESR results show that this type of intermolecular contact does not occur in solution because such a close approach would give rise to sufficient dipole–dipole coupling between the paramagnetic centers to enable the observation of $\Delta M = 2$ transitions at g ca. 4 for

(21) Dunhill, R. H.; Symons, M. C. R. *Mol. Phys.* **1968**, *15*, 105.
(22) Sawant, B. M.; Braden, G. A.; Smith, R. E.; Eaton, G. R.; Eaton, S. S. *Inorg. Chem.* **1981**, *20*, 3349.
(23) Yamanouchi, K.; Enemark, J. H. *Inorg. Chem.* **1978**, *17*, 2911.

dimers and $\Delta M = 3$ transitions at g ca. 6 for trimers. These are not observed.

The second type of intermolecular contact is of the face-to-face type between benzene rings on neighboring molecules (ring A lies over ring C). In the case of $Tc(abt)_3$, this leads to a Tc···Tc distance of 9.03 Å, and a similar distance is expected for $Re(abt)_3$. This type of intermolecular contact will give a pathway for intermolecular exchange, but at this stage it is not possible to estimate its magnitude.

The third type of intermolecular contact involves the so-called edge-to-face contacts, between the edge of a benzene ring of one molecule with the face of another benzene ring on an adjacent molecule. A calculation using the crystal structure data of Baldas et al.[1] for $Tc(abt)_3$ for the two possible edge-to-face contacts discussed by Yamanouchi and Enemark[23] gives Tc ··· Tc distances of 9.65 Å (ring A with edge B) and 11.67 Å (ring C with edge B). We therefore suggest that edge-to-face contacts give another possible pathway for intermolecular-exchange interactions, although such contacts are expected to give less electronic overlap than face-to-face contacts. A number of different trimeric structures can be suggested, all involving different combinations of face-to-face and edge-to-face contacts. The ESR evidence points to the existence of at least three and possibly four combinations, each with different magnitudes of the exchange coupling and hence different values of D. The remarkable feature of these structures is not so much that there is overlap between the π-electron clouds of the benzene rings (the distances of approach of the carbon atoms are ca. 3.5 Å) but rather that there is a high degree of delocalization of the unpaired electron from the central metal atom.

A number of examples have been reported of systems with exchange coupling between two magnetic centers separated by distances of ca. 10 Å, but most of these have been for cases where the centers belong to the same binuclear species,[24] enzyme system,[25] or are attached to the same molecular complex.[26,27] By way of contrast, there have been few observations of intermolecular-exchange interactions between paramagnetic centers where there is no distinct bonding pathway. Most of these observations have been made in the solid state.[28,29] The novel contribution of this paper is the observation of such effects in dilute frozen solution.

Registry No. I, 84943-85-1; II, 65293-30-3.

(24) Luckhurst, G. R. In "Spin Labelling—Theory and Applications"; Berliner, L. J., Ed.; Academic Press: New York, 1976; Vol. 2, pp 133–181.
(25) Boas, J. F.; Hicks, P. R.; Pilbrow, J. R.; Smith, T. D. *J. Chem. Soc., Faraday Trans. 2* **1978**, 417.
(26) Kirste, B.; Kruger, A.; Kurreck, H. *J. Am. Chem. Soc.* **1982**, *104*, 3850.
(27) Damoder, R.; More, K. M.; Eaton, G. R.; Eaton, S. S. *Inorg. Chem.* **1983**, *22*, 3738.
(28) Snaathorst, D.; Keijzers, C. P. *Mol. Phys.* **1984**, *51*, 509.
(29) Van Kalkeren, G.; Srinavasan, R.; Keijzers, C. P.; Wood, J. S.; de Boer, E. *Solid State Commun.* **1982**, *44*, 1285.

The Influence of a Second Magnesium Atom in Unsolvated Magnesium–Hydrogen Halide Reactions

Paul G. Jasien and Clifford E. Dykstra*

Contribution from the Department of Chemistry, University of Illinois, Urbana, Illinois 61801.
Received July 13, 1984

Abstract: Extensive ab initio calculations with the inclusion of electron correlation effects have been used to provide detailed information on the comparative reactions of Mg and Mg_2 with HF. Side-on reaction of HF with dimagnesium is energetically competitive with simple Mg insertion, but radical formation is a process that in the isolated molecule limit will be facilitated by involvement of a second magnesium atom. Magnesium insertion into HCl was also studied, and the transition-state structure was very much like that for insertion into HF, but the activation barrier was lower. Stabilities of dimagnesium reaction products were calculated, and these showed important metal–metal bonding. Comparison calculations on certain beryllium and calcium species show that this metal–metal bonding decreases with atomic number among the group 2 elements.

The reactive nature of elemental magnesium does not seem to be at all simple. While magnesium is generally regarded to form divalent species, we have recently found that formally univalent magnesium salts are stable by around 10–12 kcal in the isolated molecule limit.[1] (We use univalency in this instance in a very specific stoichiometric sense since these salts are of the form XMgMgX with each Mg still participating in two bonds.) The importance of magnesium reactivity, of course, has much to do with Grignard chemistry. In fact, much is still being learned about the very formation of Grignards as revealed by detailed studies on their generation at magnesium surfaces, as reported by Whitesides and co-workers.[2-5] CIDNP spectra obtained by Bickelhaupt and co-workers[6,7] have been employed to investigate radical pathways in generation reactions. While Grignard reagents are generally formed and used synthetically in solution or in slurries, recently it has been possible to study these molecules in isolated conditions, free from solvent perturbations, and in turn to probe the reactivity of elemental magnesium more directly.

Skell and Girard[8] reported the first observation of atomic magnesium reaction by way of matrix deposition. They observed reactivity of ground-state magnesium atoms with water and with alkyl halides at −196 °C. A few years later, Ault carried out matrix codeposition experiments that yielded the first spectroscopic characterization of an unsolvated Grignard species.[9] More recently, Klaubunde's codeposition studies[10] with magnesium and

(1) Jasien, P. G.; Dykstra, C. E. *Chem. Phys. Lett.* **1984**, *106*, 276.
(2) Rogers, H. R.: Hill, C. L.; Fujiwara, Y.; Rogers, R. J.; Mitchell, H. L.; Whitesides, G. M. *J. Am. Chem. Soc.* **1980**, *102*, 217. Rogers, H. R.; Deutch, J.; Whitesides, G. M. *J. Am. Chem. Soc.* **1980**, *102*, 226. Rogers, H. R.; Rogers, R. J.; Mitchell, H. L.; Whitesides, G. M. *J. Am. Chem. Soc.* **1980**, *102*, 231.
(3) Barber, J. J.; Whitesides, G. M. *J. Am. Chem. Soc.* **1980**, *102*, 239.
(4) Lawrence, L. M.; Whitesides, G. M. *J. Am. Chem. Soc.* **1980**, *102*, 2493.
(5) Hkll, C. L.; VanderSande, J. B.; Whitesides, G. M. *J. Org. Chem.* **1980**, *45*, 1020.
(6) Bodewitz, H. W. H. J.; Blomberg, C.; Bickelhaupt, F. *Tetrahadron Lett.* **1972**, 281; **1975**, 2003; *Tetrahedron* **1973**, *29*, 719; **1975**, *31*, 1053.
(7) Bodewitz, H. W. H. J.; Schaart, B. J.; Van Der Niet, J. D.; Blomberg, C.; Bickelhaupt, F.; Den Hollander, J. A. *Tetrahedron* **1978**, *34*, 2523.
(8) Skell, P. S.; Girard, J. E. *J. Am. Chem. Soc.* **1972**, *94*, 5518.
(9) Ault, B. S. *J. Am. Chem. Soc.* **1980**, *102*, 3480.

0002-7863/85/1507-1891$01.50/0